Structure and Stability of Al-Doped Boron Clusters by the Density-Functional Theory

Xiao-Juan Feng* and You-Hua Luo

Department of Physics, East China University of Science and Technology, Shanghai 200237, China

Received: August 30, 2006; In Final Form: January 25, 2007

The geometries, stabilities, and electronic properties of B_n and AlB_n clusters, up to $n = 12$, have been systematically investigated by using the density-functional approach. The results of B_n clusters are in good agreement with previous conclusions. When the Al atom is doped in B_n clusters, the lowest-energy structures of the AlB_n clusters favor two-dimensional and can be obtained by adding one Al atom on the peripheral site of the stable B_n when $n \leq 5$. Starting from $n = 6$, the lowest-energy structures of AlB_n clusters favor three-dimensional and can be described as an Al atom being capped on the B_n clusters. The average atomic binding energies, fragmentation energies, and second-order energy differences are calculated and discussed. Maximum peaks were observed for clusters of sizes $n = 5$, 8, 11, especially for the AlB_8 cluster, implying that these clusters possess relatively higher stability. The adiabatic IP and EA of AlB_n and B_n clusters are discussed and compared with some available experimental results. A distinct phenomena for AlB_n clusters is that all even n, but $n = 10$, have higher adiabatic ionization potentials than odd n.

I. Introduction

Recently, atomic clusters have drawn more and more attention[1] owning to their fundamental interest in basic research and the possibility of constructing nanostructured materials. But the history of studying clusters can be traced back to the work by Becker in 1956, in which he reported the experimental method of producing cluster beams.[2] Until the discovery of the magic number structure of the alkali metal clusters in 1984[3] and the finding of the C_{60} clusters in 1985,[4] cluster investigation was extensive. If such exotic material like C_{60} could be found, then they might have certain properties including electronic, magnetic, optical, and mechanical. Until now, there are many types of clusters investigated through theory and experiment. As for the first element of group 13, boron with an electron-deficient semimetal and a short covalent radius have been studied in several papers because of some unusual properties such as a high melting point (2300 K) and a hardness similar to that of diamond, especially for pure boron clusters. For example, Boustani investigated the geometry and electronic structures of B_n ($n \leq 14$) clusters using ab initio quantum-chemical methods in the framework of the restricted Hartree−Fock self-consistant-field approach.[5] Yang and co-workers studied the geometries, potential energy curves, and spectroscopic dissociation energies of ground and low-lying electronic states of B_2 and B_2^+ basing on the ab initio quadratic CI calculation and 6-311G basis sets.[6] The neutral and anionic forms of B_3 and B_4 were studied using photoelectron spectroscopy and ab initio calculations by Zhai and co-workers.[7] The structure and stability of B_n ($n = 5$, 6, 7) were detailedly researched by Li and Ma using MP2 and density functional theory (DFT) calculations, respectively.[8−10] B_8 clusters were investigated with MP2 and density-functional theory (DFT) methods (B3LYP and B3PW91) by Li and co-workers.[11] The equilibrium geometries, electronic and vibrational properties, and static polarizability of B_{24}, B_{24}^-, and B_{24}^+ clusters are calculated by Lau using first-principles calculations based on density-functional theory.[12] These papers give the results that for many boron clusters the planar or quasi-planar nuclear arrangement is consistently more stable than any three-dimensional structure.[5−16] These planar boron clusters indeed constitute a group of novel aromatic molecules.[17]

As far as X-doped boron clusters are concerned, there are less investigations reported. Nevertheless, Zhai and co-workers reported the electronic structure and chemical bonding of B_7Au_2 and $B_7Au_2^-$ using photoelectron spectroscopy and ab initio calculations.[18] It is well accepted that doped atoms can dramatically modify many properties of pure clusters in a variety of ways. Thus, it is necessary to study X-doped clusters' properties. In addition, Al_n ($n > 5$) clusters favor three-dimensional structures notwithstanding lying in the same column of the periodic table as boron.[19] Then, what will happen when adding one Al atom to boron clusters? To our best knowledge, there is no theoretical research about Al-doped boron clusters. So stimulated by this interesting question, a series of computational investigations has been performed on the geometry and stability of AlB_n in this paper. To acquire the influence of the Al-doped boron cluster, pure boron clusters, B_n, are also calculated using the same methods and basis sets.

This paper is arranged as follows: In Section II, we discuss computational methods briefly. Our results and discussion are presented in Section III. Finally, a conclusion is drawn in Section IV.

II. Computational Methods

Using the functionals of Becke' three-parameter hybrid exchange functional and the Lee−Yang−Parr correlation functional (B3LYP) and 6-311+G(d) basis sets, the geometry optimizations of B_n and AlB_n ($n \leq 12$) clusters are carried out by solving the Kohn−Sham equation in the framework of density-functional theory (DFT). The quality of the B3LYP/6-311+G(d) scheme for the description of B_n and AlB_n clusters was tested by calculations on the B_2 dimer. The theoretical results of the quintet B_2 dimer, including the B−B bond length (1.52 Å), vibrational frequency (1280.9 cm^{-1}), and binding

* To whom the correspondence should be addressed. E-mail: xjfeng@ecust.edu.cn.

10.1021/jp0656429 CCC: $37.00
Published on Web 03/03/2007

energy (63.5 kcal/mol), are in good agreement with the experimental values of 1.59 Å, 1051.1 cm^{-1}, and 65.5 kcal/mol,[20] respectively. In this work, first, equilibrium geometries of the B_n clusters are optimized. Second, on the basis of the optimized B_n geometries, different evolution patterns for determining the different sized AlB_n isomers, including Al-capped, Al-substituted, and Al-concaved patterns. Third, to acquire the relative stability of B_n and AlB_n clusters, binding energy, fragmentation energy, gaps between the HOMO (highest occupied molecular orbital) and LUMO (lowest unoccupied molecular orbital), and second-order difference of total energies are calculated. Moreover, the electronic properties such as ionization potential and electron affinity are also investigated. All calculations are carried out with the GAUSSIAN 03 program package.[21]

III. Results and Discussions

A. Growth Behavior of Different Sized Al-Doped Boron Clusters. Using the computation scheme described in Section II, we have explored a number of low-lying isomers and determined the lowest-energy structures for AlB_n clusters up to $n = 12$. The lowest-energy structures and some low-lying metastable isomers are shown in Figure 1. Using the same computation scheme, we reoptimized the pure B_n clusters for the purpose of comparison, which have been investigated extensively by both ab initio and density-functional approaches.[5−16] Only the lowest-energy structures for B_n are shown in Figure 1.For AlB_2 and AlB_3, the lowest-energy structures can be obtained by directly adding one Al atom to the pure B_n clusters. A isosceles triangle (C_{2v}), with a total energy of −291.94155 hartree, was found as the lowest-energy structure for AlB_2 (2a in Figure 1), with two Al−B bonds of 2.02450 Å and one B−B bond of 1.55329 Å, respectively. The linear chain (C_s or $D_{\infty h}$) isomers (2b and c in Figure 1) are higher in energy than the lowest-energy structure at 0.907 eV and 4.028 eV. In the case of $n = 3$, the most stable geometry of B_3 is a closed equilateral triangular structure (D_{3h}) ($3a_0$ in Figure 1) with a total energy of −74.29827 hartree. Adding one Al atom directly to the B_3, the lowest-energy structure of AlB_3 (3a in Figure 1) can be obtained with the C_{2v} symmetry and −316.79018 hartree in total energy. Another low-lying isomer for AlB_3 is a trigonal pyramid with C_{3v} symmetry (3b in Figure 1), 0.152 eV higher than the lowest-energy structure. When one B atom in the B_4 ($4a_0$ in Figure 1) is substituted by Al, a new structure is formed, but 0.344 eV higher than the lowest-energy structure.

The lowest-energy structure for B_4 is a planar rhombus ($4a_0$ in Figure 1) with a total energy of −99.15755 hartree, which can be generated by capping the B atom on the peripheral site of the stable B_3 frame, and this is in agreement with previous calculations.[7] Adding one Al atom on the peripheral site of the stable B_4 and having a little distortion, the lowest-energy structure of AlB_4 can be obtained with C_s symmetry and −341.63852 hartree in total energy (4a in Figure 1). The other two low-lying isomers (4b and c in Figure 1) can also be obtained by adding one Al atom on the peripheral site of the stable B_4, but they are 0.169 eV and 0.924 eV higher in total energy than the lowest-energy structure. It is strange that there is no such pyramid structure for AlB_4, which is unlike other AlB_n clusters.

For $n = 5$, the planar five-membered ring structure with C_{2v} symmetry is the lowest in energy (−124.00303 hartree), in agreement with the results obtained by Boustani [5] and Qian Shu Li et al.[8] For AlB_5, the lowest-energy structure can be obtained by adding one Al atom on the peripheral site of the stable B_5 and also having a little distortion, with C_s symmetry and −341.63852 hartree in total energy (5a in Figure 1). There are other isomers for AlB_5 (5b−f in Figure 1); for example, when one B atom in the B_6 ($6a_0$ in Figure 1) is substituted by Al atom, a new structure of AlB_5 is formed and is only 0.094 eV

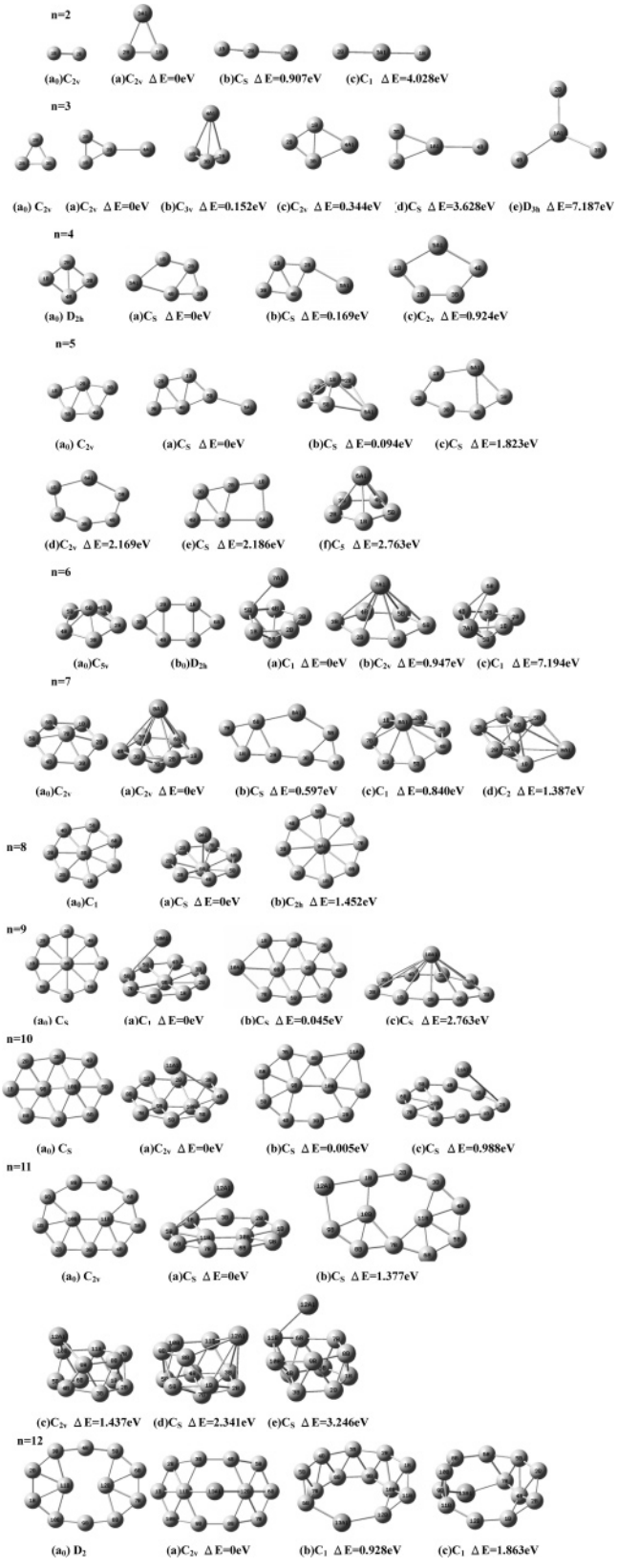

Figure 1. Lowest-energy and low-lying structures of AlB_n ($n = 2-12$) clusters and lowest-energy structures of pure B_n ($n = 2-12$) clusters.

TABLE 1: Binding Energy, Shortest Al−B and B−B Bond Lengths, and Electronic State of AlB_n and B_n Clusters for the Lowest-Energy Structures

cluster	E_b (eV)	R_{Al-B} (Å)	R_{B-B} (Å)	state	cluster	E_b (eV)	R_{B-B} (Å)	state
AlB_2	2.12772	2.02449	1.55329	$^2A'$	B_2	1.42338	1.51842	$^5\Sigma$
AlB_3	2.87330	2.18768	1.51576	$^1A'$	B_3	2.86484	1.54785	$^2A'$
AlB_4	3.31902	2.04009	1.53391	$^2A'$	B_4	3.49849	1.52290	$^1A'$
AlB_5	3.63158	2.20691	1.55538	$^1A'$	B_5	3.80368	1.55347	$^2A'$
AlB_6	3.76053	2.25628	1.59443	^2A	B_6	3.91179	1.60960	^1A
AlB_7	4.01166	2.48126	1.54286	^1A	B_7	4.21547	1.56871	^2A
AlB_8	4.29030	2.12139	1.54292	^2A	B_8	4.38321	1.51049	$^1A'$
AlB_9	4.30470	2.49334	1.51297	^1A	B_9	4.43735	1.50905	^2A
AlB_{10}	4.39923	2.71622	1.61932	^2A	B_{10}	4.60612	1.58107	^1A
AlB_{11}	4.46480	2.66108	1.52968	^1A	B_{11}	4.66904	1.54206	^2A
AlB_{12}	4.46280	2.09394	1.56945	^2A	B_{12}	4.63738	1.50672	^1A

higher than the lowest-energy structure. Because the lowest-energy structures of the AlB_{6-12} clusters are three-dimensional, $n = 5$ can be seen as a transition point from a two-dimensional to a three-dimensional structure.

As far as $n = 6$, there are two stable structures with little difference in total energy for B_6. One is a pentagonal pyramid structure with C_{5v} symmetry ($6a_0$ in Figure 1). The other is a cyclic planar structure with D_{2h} symmetry ($6b_0$ in Figure 1). Furthermore, the energy for $6a_0$ in Figure 1 is a little higher than that for $6b_0$ in Figure 1. But using the vibrational frequency results, there is a negative vibrational frequency for the 6b structure; therefore, the 6b structure is not the ground state. The true most stable structure is the 6a structure and is in agreement with the results obtained by J. Niu et al.[22] For AlB_6, the lowest-energy structure is a pentagonal bipyramid, with C_1 symmetry (6a in Figure 1), which can be seen on the Al atom occupying a site on the vertex. When the Al atom occupies a site on the pentagonal ring, other AlB_6 (6c in Figure 1) isomers can be obtained, but the former one is much lower in energy by 7.194 eV. A hexagonal pyramid structure with C_{2v} symmetry (6b in Figure 1) is only 0.947 eV higher than the ground state in total energy, and it can be seen as a substitutional structure of B_7 ($7a_0$ in Figure 1).

For B_7, we obtained a hexagonal pyramid with C_{2v} symmetry ($7a_0$ in Figure 1) and in agreement with the result obtained by Q. S. Li et al.[10] If you turn over the B_7 and place the Al atom above that, then the lowest-energy structure for AlB_7 can be obtained with a hexagonal bipyramid and C_{2v} symmetry (7a in Figure 1). The shortest Al−B bond length occurs for 2B−8Al and 5B−8Al at 2.48126 Å. The distance of 1B−2B and 4B−5B is shortest among the B−B bond lengths at 1.54286 Å. Several other isomers were considered, including one plane structure and two 3D structures (7b−d in Figure 1). The total energy is 0.597, 0.840, and 1.387 eV higher than the lowest-energy structure, respectively.

For B_8, the lowest-energy structure is a heptagon with a central atom and C_1 symmetry ($8a_0$ in Figure 1). Our heptagon structure agrees with the theoretical predictions by Boustani[5] and Zhai et al.[23] Two isomers for AlB_8 are shown in Figure 1 (8a and b). 8a is the lowest-energy structure and can be obtained like AlB_7. The most interesting thing about AlB_8 is that the structure is very much like an umbrella. The shortest B−Al bond length belongs to 8B−9Al at 2.12139 Å. Another isomer 8b is a substitutional structure of B_9 ($9a_0$ in Figure 1) and is 1.542 eV higher than 8a in total energy.

An octagon with a central atom and C_s symmetry ($9a_0$ in Figure 1) is obtained for B_9. Our octagon structure agrees with the result by Zhai et al.[23] Like AlB_7 and AlB_8, the lowest-energy structure can be obtained for AlB_9 (9a in Figure 1). The shortest B−Al bond length also like AlB_8 belongs to 9B−10Al at 2.49334 Å. It should be noted that another isomer (9b in Figure 1) is only 0.045 eV higher than the lowest-energy structure in total energy. It can be seen as a substitutional structure of B_{10} ($10a_0$ in Figure 1) with C_s symmetry.

The most stable structure of B_{10} has two dovetailed hexagonal pyramids ($10a_0$ in Figure 1) but with two tops reversed. This structure agrees with the theoretical prediction by Boustani.[5] Like AlB_{7-9}, place the Al atom above that, and the lowest-energy structure for AlB_{10} can be obtained with C_{2v} symmetry (10a in Figure 1). The shortest Al−B bond length occurs for 10B−12Al at 2.66108 Å. The distance of 6B−7B and 4B−5B is shortest among the B−B bond lengths at 1.52968 Å. The other two isomers are also shown in Figure 1 (10b and c in Figure 1). Furthermore, there is only a 0.005 eV difference between 10a and 10b. 10b can also be seen as a substitutional structure of B_{11} ($11a_0$ in Figure 1) with C_s symmetry.

For B_{11}, the lowest-energy structure ($11a_0$ in Figure 1) contains two connected subunits, the shallow hexagonal and heptagonal pyramids. Our result agrees with the theoretical prediction by Boustani.[5] The shortest B−B bond length is 1.54206 Å for B8−B9. Using the same method, the lowest-energy structure for AlB_{11} can be obtained with C_s symmetry (11a in Figure 1). The distance of 10B−12Al is the shortest among the B−Al bonds at 2.66108 Å. The shortest B−B bond length occurs for 6B−7B at 1.52968 Å. The other four isomers are also shown in Figure 1 (10b and c in Figure 1). However, there is much difference (at least 1.377 eV) between 11a and other isomers. 11b can also be seen as a substitutional structure but with some retortion of B_{12} ($12a_0$ in Figure 1) with C_s symmetry.

For B_{12}, the lowest-energy structure ($12a_0$ in Figure 1) consists of a dimer surrounded by 10 atoms and can be considered as containing two dovetailed shallow heptagonal pyramids. This structure agrees with the theoretical prediction by Boustani.[5] The shortest B−B bond length is 1.50672 Å for B5−B6. Using the same method, the lowest-energy structure for AlB_{12} can be obtained with C_{2v} symmetry (12a in Figure 1). The distance of 11B,12B−13Al is the shortest among the B−Al bond lengths at 2.09394 Å. The shortest B−B bond length occurs for 2B−3B, 4B−5B, 7B−8B, and 9B−10B at 1.56945 Å.

According to the discussion above, it is concluded that the lowest-energy structures of AlB_n can be obtained by adding one Al atom on the peripheral site of the stable B_n and favor two-dimensional when $n \leq 5$. From $n = 6$, the lowest-energy structures of AlB_n clusters can be described as an Al atom being capped on the B_n clusters and favor three-dimensional.

B. Relative Stability and Electronic Properties. *Relative Stability.* The relative stability of the different sized clusters can be predicted by calculating the average binding energy and fragmentation energy. The average binding energy for the B_n and AlB_n clusters can be defined by the following formula $E_b(n) = [nE_T(B) - E_T(B_n)]/n$, $E'_b(n) = [nE_T(B) + E_T(Al) - E_T(AlB_n)]/n + 1$, where $E_T(B)$, $E_T(Al)$, $E_T(AlB_n)$, and $E_T(B_n)$ represent the total energies of the most stable B, Al, AlB_n, and B_n clusters, respectively. From Figure 2, it can be seen that the binding energy generally increases with cluster size. Thus, the clusters can continue to gain energy during the growth process. Furthermore, both curves reveal the same size dependence with enhanced stability at $n = 5$, 8, and 11. This result indicates that the stability of AlB_n can be related to the stability of pure B_n.

In addition to the binding energy, the size dependence of the fragmentation energies of the B_n and AlB_n clusters is also investigated. The fragmentation energy can be defined by the following formula $E_F(n) = E_T(B) + E_T(B_{n-1}) - E_T(B_n)$, E'_F-

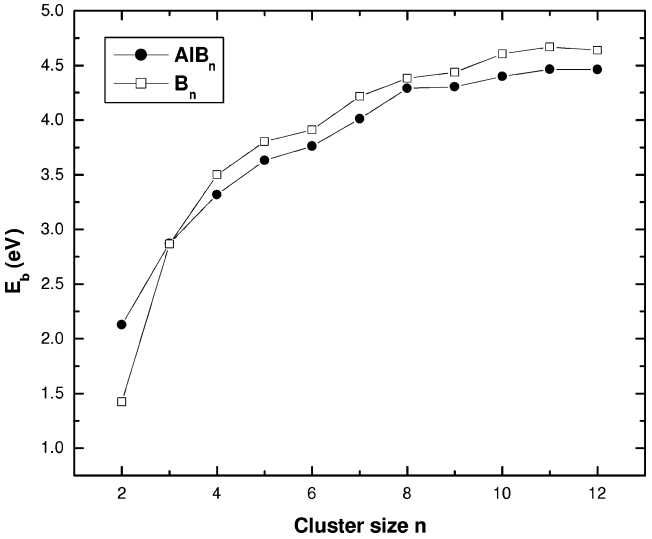

Figure 2. Size dependence of the binding energy per atom of AlB_n and B_n clusters.

TABLE 2: Adiabatic Ionization Potential (IP), Electron Affinity(EA), HOMO−LUMO Gap, and Atomic Charges at the Al Atom of AlB_n Clusters for the Lowest-Energy Structures

cluster	IP (eV)	EA (eV)	gap (eV)
AlB_2	8.430	2.170	2.125
AlB_3	7.910	1.783	2.603
AlB_4	8.144	2.555	2.347
AlB_5	7.330	2.116	1.965
AlB_6	8.216	1.229	2.355
AlB_7	7.741	3.031	2.064
AlB_8	8.954	3.196	2.383
AlB_9	7.682	2.561	4.633
AlB_{10}	7.448	2.515	1.874
AlB_{11}	7.838	2.309	2.464
AlB_{12}	8.172	3.661	1.791

$(n) = E_T(AlB_{n-1}) + E_T(B) - E_T(AlB_n)$, where $E_T(B)$, $E_T(B_{n-1})$, $E_T(AlB_{n-1})$, $E_T(Al)$, $E_T(AlB_n)$, and $E_T(B_n)$ represent the total energies of the most stable B, B_{n-1}, AlB_{n-1}, $E_T(Al)$, $E_T(AlB_n)$, and $E_T(B_n)$ clusters, respectively.As shown in Figure 3, the lowest fragmentation energies appear at $n = 6, 9$. This indicates that B_6, B_9, AlB_6, and AlB_9 clusters are less stable than their neighbors, which can also be obtained from Figure 2. The local peaks of $E_F(n)$ appear at the sizes of 7 and 10. However, when Al is doped in the B_n clusters, this situation is obvious. As can be seen from Figure 3, the local maxima of $E'_F(n)$ appear at the sizes of 5, 8, and 10.

In cluster physics, the second-order difference of cluster energies, $\Delta_2E(n) = E(n+1) + E(n-1) - 2E(n)$, is a sensitive quantity that reflects the relative stability of the clusters.[24] Figure 4 shows the second-order difference of cluster energies, $\Delta_2E(n)$, as a function of the cluster size. Maxima are found at $n = 5$, 8, and 11, indicating that these clusters possess higher stability, which is consistent with the trend of binding energies shown in Figure 2.

As shown in Figure 5, the HOMO−LUMO (highest occupied molecular orbital-lowest unoccupied molecular orbital) gaps of AlB_n are usually smaller than those of B_n clusters except at $n = 8$, 9, 11. The gaps are close to each other at $n = 3$, 7. It should be pointed out that AlB_9 has a very large gap (4.633 eV); maybe there is other important information. Further investigation will be done in our future research. We do not find a strong correlation between the HOMO−LUMO gaps and the energetic stability of the clusters.

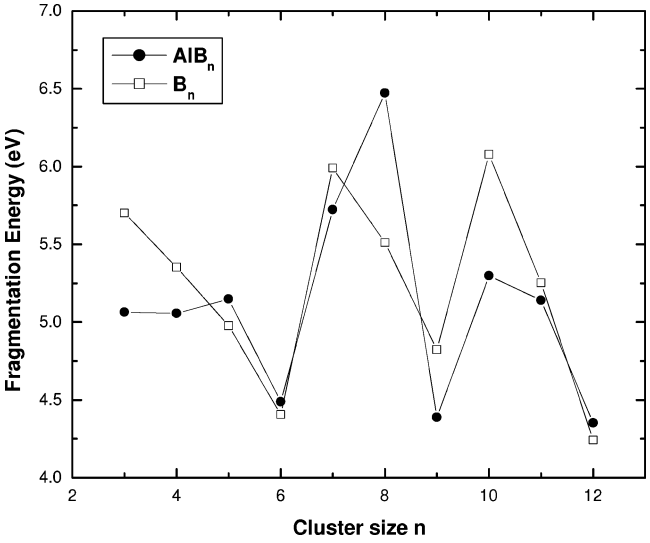

Figure 3. Size dependence of the fragmentation energy of AlB_n and B_n clusters.

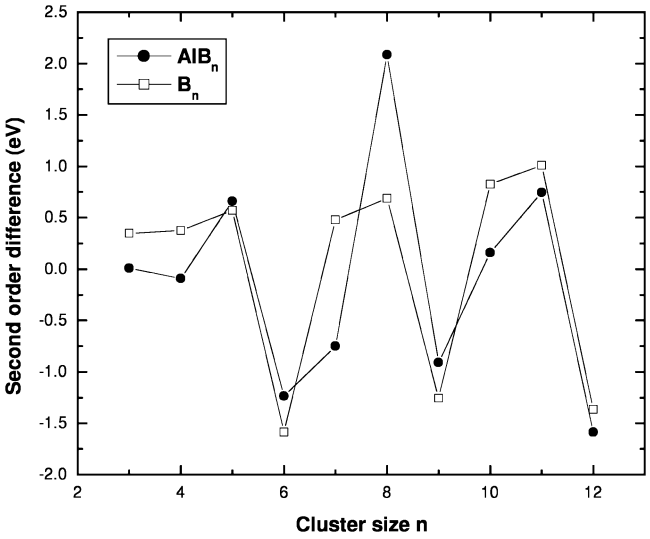

Figure 4. Second-order differences energy of neutral AlB_n and B_n clusters.

Electronic Properties. The ionization potential (IP) is an important parameter to understand the stability toward ejecting out one electron from its HOMO energy level to the continuum. Usually, there are three types of IP: Koopmans IP, vertical IP and adiabatic IP. Koopmans IP is the HOMO energies, vertical IP is the energy difference between the neutral and ionic clusters at the neutral equilibrium geometry, and adiabatic IP is the energy difference between the neutral and ionic clusters at their respective equilibrium geometry. In this work, the adiabatic IP of AlB_n and B_n clusters for their lowest-energy structures are calculated and compared with some available experiment results, as shown in Figure 6. Both our theory and previous experiment suggest a maximum in the IP's for B_n clusters at B_3. (The previous experimental result of IP for B_3 is 14.0 eV.)[25] For AlB_n clusters, AlB_8 has the largest adiabatic ionization potential, corresponding to its higher stability. A distinct phenomena for AlB_n clusters is that all even n but $n = 10$ have higher adiabatic ionization potentials than odd n.

The adiabatic electron affinities (A.E.A) of AlB_n and B_n clusters for their lowest-energy structures are also calculated and compared with some available experimental results,[7,23,26,27] as shown in Figure 7. The theoretical data for $B_{3-5,7-9}$ have the same tendency as the experimental data except for B_8. Unlike

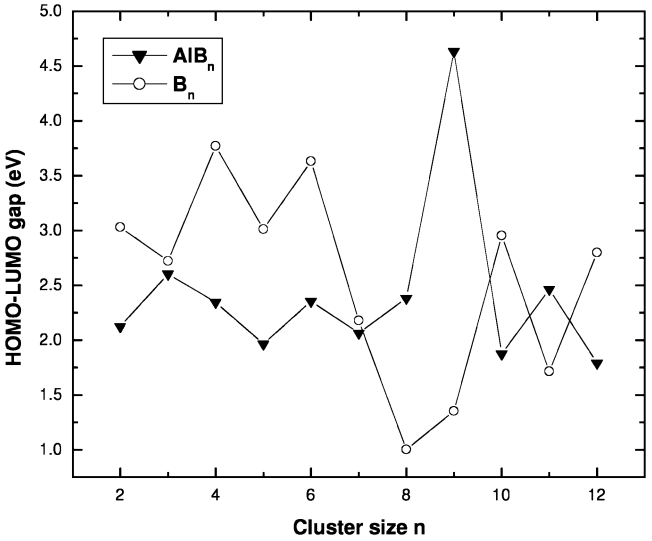

Figure 5. Size dependence of HOMO−LUMO of AlB_n and B_n clusters.

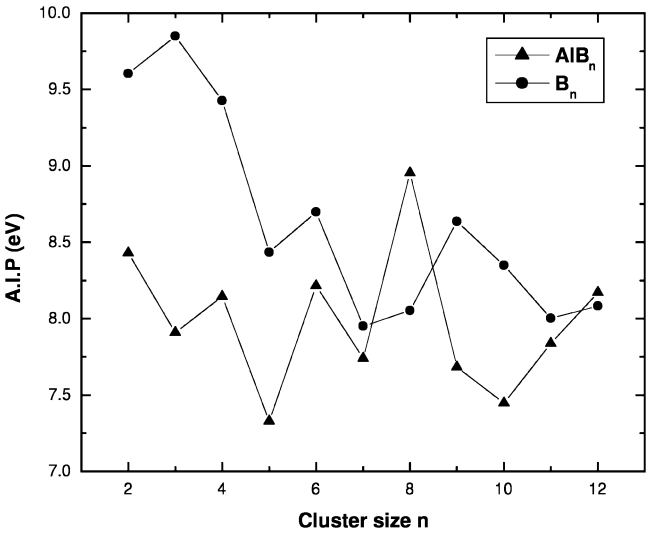

Figure 6. Comparison of the adiabatic ionization potentials between AlB_n and B_n clusters.

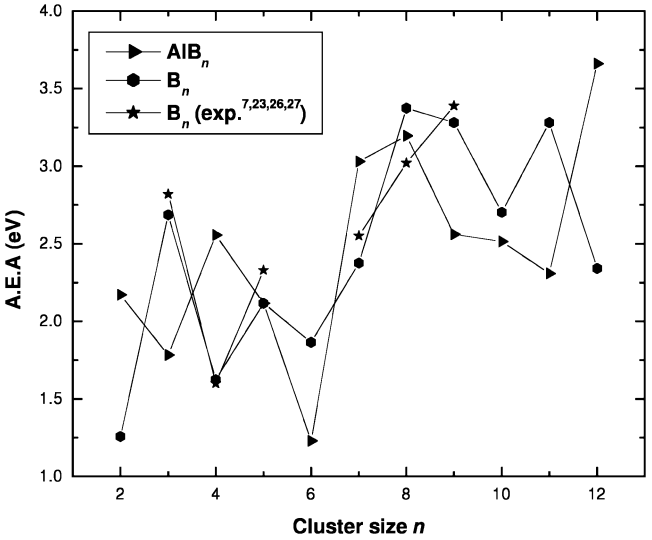

Figure 7. Comparison of the adiabatic electron affinity between AlB_n and B_n clusters.

the ionization potential, there is no distinct rule for electron affinities. From Figure 7, we can see that the A.E.A for some sizes of AlB_n clusters are larger than those of B_n clusters, for example, $n = 2$, 4, 7, 12. From 8 to 11, the A.E.A of B_n are all larger than those of AlB_n.

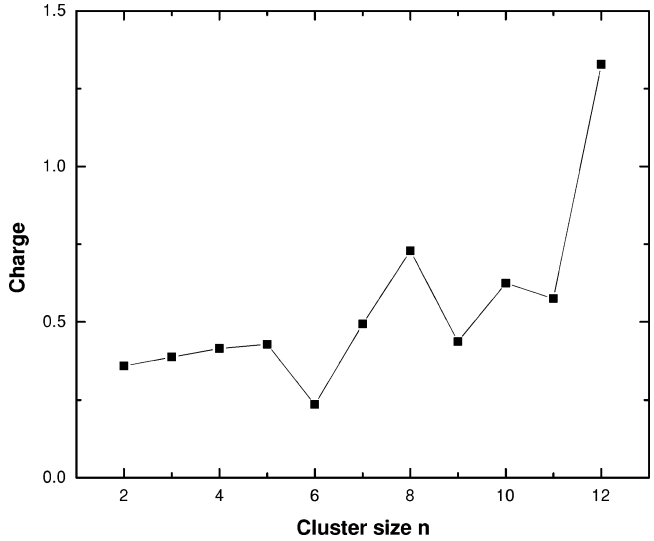

Figure 8. Size dependence of atomic charges of Al atom of AlB_n clusters.

Mulliken population analysis for the lowest-energy structures are performed, and the atomic charges of the Al atom of the AlB_n clusters are plotted in Figure 8. Charge always transfers from the Al to the B atom with the increase of size and indicates that Al acts as an electron donor in all AlB_n clusters. The local minima for the different sized AlB_n clusters can be found at 6 and 9; this finding provides support of our calculated relative stability by aid of the calculated fragmentation energy. From $n = 2$ to $n = 5$, there is about 0.4e charge transfer. $n = 6$ is a local minimum. From $n = 6$ to $n = 8$, the charge transfer from the Al atom to the B atom generally increases. $n = 9$ is anther local minimum. There is an abrupt increase from 11 to 12.

To gain more information of electronic properties, we consider the results of natural bond analysis (NBO),[28] which is based on the use of localized orbitals constructed from the occupancy-weighted symmetric orthogonalized natural atomic orbitals and provides effective electronic configurations for each atom in a cluster. AlB_7, AlB_8, and AlB_9 are chosen as examples. In the lowest-energy structures of AlB_7 (7a in Figure 1), AlB_8 (8a in Figure 1), and AlB_9 (9a in Figure 1), the effective atomic configurations of Al are (core)$(3s^{1.71}3p^{0.48})$, (core)$(3s^{0.96}3p^{0.97})$, and (core)$(3s^{1.93}3p^{0.38})$, respectively. It can be easily seen that the Al atom in the AlB_8 cluster offers more electrons to share with B atoms than that in the AlB_7 and AlB_9 clusters. Therefore, the electrostatic interaction between the Al atom and the B atoms of the AlB_8 cluster is stronger than that for the AlB_7 and AlB_9 clusters. This conclusion can further illuminate that the AlB_8 cluster is more stable than the AlB_7 and AlB_9 clusters. At last, it should be pointed out that the Al atom in the AlB_{12} cluster also offers more electrons to share with B atoms, but it is not a maximum in Figure 4. The possible reason is that the isomers for AlB_{13} are not enough. Further investigation will be done for the XB_{12} cluster in our future research.

IV. Conclusions

The growth behaviors, stabilities, and electronic properties of the B_n and AlB_n, n up to 12, clusters are investigated theoretically at the B3LYP level by employing 6-311+G(d) basis sets. The lowest-energy structures of AlB_n can be obtained by adding one Al atom on the peripheral site of the stable B_n

when $n \leq 5$. From $n = 6$, the lowest-energy structures of AlB_n clusters can be described as Al being capped on the B_n clusters and favor three-dimensional structures. The average atomic binding energies, fragmentation energies, and second-order energy differences are calculated and discussed. From the analysis of second-order energy difference, AlB_n clusters at $n = 5$, 8, 11 possess relatively higher stability. The results of natural bond analysis (NBO) indicate that the Al atom in the AlB_8 cluster offers more electrons to share with B atoms than that in the AlB_7 and AlB_9 clusters. Therefore, the electrostatic interaction between the Al atom and the B atoms for the AlB_8 cluster is stronger than that for the AlB_7 and AlB_9 clusters. This conclusion can further illuminate that the AlB_8 cluster is more stable than the AlB_7 and AlB_9 clusters. The adiabatic IP and EA of the AlB_n and B_n clusters for their lowest-energy structures are discussed. For the AlB_n clusters, all even n, but $n = 10$, have higher adiabatic ionization potentials than odd n. There is no distinct rule for AlB_n in electron affinities.

Acknowledgment. This work is financially supported in part by the National Natural Science Foundation of China (Grant No. 10174086) and the Foundation for the research starting of East China University of Science and Technology (Grant No. YK0142109).

References and Notes

(1) *Clusters of Atoms and Molecules I*; Haberland, H, Ed.; Springer-Verlag: Berlin, 1995.

(2) Becker, E. W. *Z. Phys*. **1956**, *146*, 333.

(3) Knight, W. D.; Clemenger, K.; de Heer, W. A.; Saunders, W. A.; Chou, M. Y.; Cohen, M. L. *Phys. Rev. Lett*. **1984**, *52*, 2141.

(4) Kroto, H. W.; Heath, J. R.; O' Brian, S. C.; Curl, R. F.; Smalley, R. E. *Nature* (*London*) **1985**, *318*, 162.

(5) Boustani, I. *Phys. Rev. B* **1997**, *55*, 16426.

(6) Yang, C. L.; Zhu, Z. H.; Wang, R.; Liu, X. Y. *J. Mol. Struct.: THEOCHEM* **2001**, *548*, 47.

(7) Zhai, H.-J.; Wang, L.-S.; Alexandrova, A. N.; Boldyrev. A. I.; Zakrzewski, V. G. *J. Phys. Chem. A* **2003**, *107*, 9319.

(8) Li, Q. S.; Jin, H. W. *J. Phys. Chem. A* **2002**, *106*, 7042.

(9) Ma, J.; Li, Z. H; Fan, K. N.; Zhou, M, F. *Chem. Phys. Lett*. **2003**, *372*, 708.

(10) Li, Q. S.; Gong, L. F.; Gao, Z. M. *Chem. Phys. Lett*. **2004**, *390*, 220.

(11) Li, Q. S.; Zhao, Y.; Xu, W. G.; Li, N. *Int. J. Quantum Chem*. **2004**, *101*, 219.

(12) Lau, K. C.; Deshpande, M.; Patt, R.; Pandey, R. *Int. J. Quantum Chem*. **2005**, *103*, 866.

(13) Ricca, A.; Bauschlicher, C. W. *J. Chem. Phys*. **1996**, *208*, 233.

(14) Wyss, M.; Riaplov, E.; Batalov, A.; Maier, J. P.; Weber, T.; Meyer, W.; Rosmus, P. *J. Chem. Phys*. **2003**, *119*, 9703.

(15) Cias, P.; Araki, M.; Denisov, A.; Maier, J. P. *J. Chem. Phys*. **2004**, *121*, 6776.

(16) Linguerri, R.; Navizet, I.; Rosmus, P.; Carter, S.; Maier, J. P. *J. Chem. Phys*. **2005**, *122*, 034301.

(17) Aihara, J. I.; Kanno, H.; Ishida, T. *J. Am. Chem. Soc*. **2005**, *127*, 13324.

(18) Zhai, H. J.; Wang, L. S.; Zubarev, D. Y.; Boldyrev, A. I. *J. Phys. Chem. A* **2006**, *110*, 1689.

(19) Akola, J.; Häkkinen, H.; Manninen, M. *Phys. Rev. B* **1998**, *58*, 3601.

(20) Rosen, B. *Spectroscopic Data Relative to Diatomic Molecules*; Pergamon Press: Oxford, 1970.

(21) Frisch, M. J.; Trucks, G. W.; Schlegel, H. B.; Scuseria, G. E.; Robb, M. A.; Cheeseman, J. R.; Montgomery, J. A., Jr.; Vreven, T.; Kudin, K. N.; Burant, J. C.; Millam, J. M.; Iyengar, S. S.; Tomasi, J.; Barone, V.; Mennucci, B.; Cossi, M.; Scalmani, G.; Rega, N.; Petersson, G. A.; Nakatsuji, H.; Hada, M.; Ehara, M.; Toyota, K.; Fukuda, R.; Hasegawa, J.; Ishida, M.; Nakajima, T.; Honda, Y.; Kitao, O.; Nakai, H.; Klene, M.; Li, X.; Knox, J. E.; Hratchian, H. P.; Cross, J. B.; Bakken, V.; Adamo, C.; Jaramillo, J.; Gomperts, R.; Stratmann, R. E.; Yazyev, O.; Austin, A. J.; Cammi, R.; Pomelli, C.; Ochterski, J. W.; Ayala, P. Y.; Morokuma, K.; Voth, G. A.; Salvador, P.; Dannenberg, J. J.; Zakrzewski, V. G.; Dapprich, S.; Daniels, A. D.; Strain, M. C.; Farkas, O.; Malick, D. K.; Rabuck, A. D.; Raghavachari, K.; Foresman, J. B.; Ortiz, J. V.; Cui, Q.; Baboul, A. G.; Clifford, S.; Cioslowski, J.; Stefanov, B. B.; Liu, G.; Liashenko, A.; Piskorz, P.; Komaromi, I.; Martin, R. L.; Fox, D. J.; Keith, T.; Al-Laham, M. A.; Peng, C. Y.; Nanayakkara, A.; Challacombe, M.; Gill, P. M. W.; Johnson, B.; Chen, W.; Wong, M. W.; Gonzalez, C.; Pople, J. A. *Gaussian 03*, revision A.1; Gaussian, Inc.: Wallingford, CT, 2004.

(22) Niu, J.; Rao, B. K.; Jena, P. *J. Chem. Phys*. **1997**, *107*, 132.

(23) Zhai, H. J.; Wang, L. S.; Alexandrova, A. N.; Boldyrev. A. I. *Angew. Chem., Int. Ed*. **2003**, *42*, 6004.

(24) Wang, J. L.; Wang, G. H.; Zhao, J. J. *Phys. Rev. B* **2001**, *64*, 205411.

(25) Hanley, L.; Whitten, J. L. Anderson, S. L. *J. Phys. Chem*. **1988**, *92*, 5803.

(26) Zhai, H. J.; Wang, L. S.; Alexandrova, A. N.; Boldyrev. A. I. *J. Chem. Phys*. **2002**, *117*, 7917.

(27) Alexandrova, A. N.; Boldyrev, A. I.; Zhai, H. J.; Wang, L. S. *J. Phys. Chem. A* **2004**, *108*, 3509.

(28) Reed, A. E.; Curtiss, L. A.; Weinhold, F. *Chem. Rev*. **1988**, *88*, 899.